Tetra(4-methoxyphenyl)phosphonium Iodide: A Twinned Crystal Built Up with Three-Dimensional Octupolar Nonlinear Optical Chromophores

ARTICLE *in* CHEMISTRY OF MATERIALS · MARCH 2000

Impact Factor: 8.35 · DOI: 10.1021/cm991155c

6 AUTHORS, INCLUDING:

Patrick Masson
Institut de Physique et Chimie des Matériaux …
35 PUBLICATIONS **549** CITATIONS
SEE PROFILE

Jean-François Nicoud
University of Strasbourg
165 PUBLICATIONS **4,501** CITATIONS
SEE PROFILE

Tetra(4-methoxyphenyl)phosphonium Iodide: A Twinned Crystal Built Up with Three-Dimensional Octupolar Nonlinear Optical Chromophores

Cyril Bourgogne,[†] Yvette Le Fur,[‡] Patrick Juen,[‡] Patrick Masson,[†] Jean-François Nicoud,*[,†] and René Masse*[,‡]

Groupe des Matériaux Organiques, Institut de Physique et Chimie des Matériaux de Strasbourg, CNRS et Université Louis Pasteur (UMR 7504), 23 rue du Loess, 67037 Strasbourg-Cedex, France, and Laboratoire de Cristallographie associé à l'Université Joseph Fourier, CNRS, BP166, 38042 Grenoble-Cedex, France

Received October 11, 1999. Revised Manuscript Received January 10, 2000

The tetra(4-methoxyphenyl)phosphonium iodide $C_{28}H_{28}O_4PI$ (MOPPI) is a crystal built up with quasi octupolar tetrahedral chromophores having quadratic nonlinear optical (NLO) properties. The calculated values of the highest tensor component β_{xyz} for the hyperpolarizable chromophore, in its most stable S_4 geometry, vary from 4.23 to 9.23 $\times$ 10^{-30} esu, depending on the methods of calculation. Given the linear absorption maximum at 255 nm, this reveals a good hyperpolarizability−transparency tradeoff. The crystal is twinned by merohedry. The crystal structure was solved until a reliability factor $R = 0.048$ using 2189 untwinned reflections. The material crystallizes in the noncentrosymmetric orthorhombic space group $P2_12_12_1$ with $Z = 4$ and the unit cell parameters $a = b = 10.131(3)$ Å, $c = 25.682(6)$ Å. The cation−anion arrangement corresponds to a NaCl-type model weakly distorted. Signal of second harmonic of a crystalline powder at 1.06 μm is nearly equivalent to that of urea.

Introduction

In the engineering of crystalline materials for quadratic nonlinear optics most attention was paid, until now, to the use of quasi one-dimensional (1D) polar chromophores and the means directing their noncentrosymmetric assemblies.[1] If it is true that polar rodlike molecules such as nitroanilines and donor−acceptor stilbene derivatives generally tend to set up antiparallel arrangements, this situation can often be hindered by energetic intermolecular hydrogen bonds or metal−ligand bonds. Purely polar or herringbone structures resulting of such strong interactions crystallize with needle or platelet morphologies which are very difficult to grow with acceptable size for optical applications. Another drawback of the use of rodlike 1D chromophores is the small off-diagonal components of their hyperpolarizability β tensor; therefore, the contribution of a unique high coefficient β_{xxx} (x being the direction of the molecular charge-transfer axis) to the macroscopic tensor induces a unique high value for the quadratic susceptibility $\chi^{(2)}$ in optimized crystal structures.[2] Such a situation limits the optical applications (parametric effects) since we have to take into account simultaneously a configuration of polarized beams, a high $\chi^{(2)}$ value, and a noncritical phase matching. To overcome these drawbacks Zyss has proposed and justified the design of new NLO crystalline materials based on the three-dimensional packing of two-dimensional (2D) or three-dimensional (3D) octupolar chromophores.[3] In such chromophores the cancellation of the dipole moments in the excited as well as ground states occurs.[3c] These molecular or ionic entities which preserve a nonzero β tensor with several useful coefficients present an intramolecular charge-transfer (ICT) described by pure octupolar point groups: orthorhombic D_2, hexagonal D_{3h}, and cubic T_d (even if the actual molecular symmetry is often reduced by steric interactions). Such molecular properties can be exploited in an octupolar NLO material by adequate photoinduced orientation of the chromophores in an amorphous matrix (octupolar[4] or even one-dimensional[5]). The other way remains the noncentrosymmetric packing of the hyperpolarizable octupolar chromophore in the solid state. The crystal of triaminotrinitrobenzene (TATB) built up with chromophores of D_{3h} symmetry illustrates the crystal design with two-dimensional CT states.[6] Few crystalline ma-

* Authors for correspondence. E.mail: nicoud@michelangelo.u-strasbg.fr and masse@labs.polycnrs-gre.fr.
† CNRS et Université Louis Pasteur (UMR 7504).
‡ CNRS et Université Joseph Fourier.

(1) (a) *Nonlinear Optical Properties of Organic Molecules and Crystals*; Chemla, D. S., Zyss, J., Eds.; Academic Press: Orlando, 1987; Vols. I and II. (b) Prasad, P. N.; Williams, D. J. *Introduction to Nonlinear Optical Effects in Molecules and Polymers*; Wiley-Interscience: New York, 1991. (c) *Materials for Nonlinear Optics: Chemical Perspectives*; Marder, S. R., Sohn, J. E., Stucky, G. D., Eds.; ACS Symposium Series 455; American Chemical Society: Washington, DC, 1991. (d) *Molecular Nonlinear Optoelectronics: Materials, Physics and Devices*; Zyss, J., Ed.; Academic Press: San Diego, London, 1994.

(2) Zyss, J.; Oudar, J. L. *Phys. Rev.* **1982**, *A26*, 2028.

(3) (a) Zyss, J. *Nonlinear Opt.* **1991**, *1*, 3. (b) Zyss, J. *J. Chem. Phys.* **1993**, *98*, 6583. (c) Zyss, J.; Ledoux, I. *Chem. Rev.* **1994**, *94*, 77. (d) Zyss, J.; Ledoux, I.; Nicoud, J.-F. Advances in molecular engineering for quadratic nonlinear optics. *Molecular Nonlinear Optoelectronics: Materials, Physics and Devices*; Zyss, J., Ed.; Academic Press: Boston, 1994; pp 180−193. (e) Zyss, J.; Brasselet, S.; Thalladi, V. R.; Desiraju, G. R. *J. Chem. Phys.* **1998**, *109*, 658.

(4) Fiorini, C.; Charra, F.; Nunzi, J.-M.; Samuel, I.; Zyss, J. *Opt. Lett.* **1995**, *20*, 2469.

(5) Brasselet, S.; Zyss, J. *J. Opt. Soc. Am. B* **1998**, *15*, 257.

10.1021/cm991155c CCC: $19.00
Published on Web 03/24/2000

terials built from this kind of planar octupolar molecules have been described.[7] In contrast NLO octupolar chromophores with three-dimensional CT states, for which only β_{xyz} is significant, have attracted little attention in crystal engineering. With regard to the structural point of view, the engineering of such octupolar crystals can be considered as a research of noncentrosymmetric packing of spherical entities, a field of investigation well explored in inorganic structural chemistry: for instance, crystals derived of zinc blende structure as GaAs ($F\bar{4}3m$), $CdHg(SCN)_4$ ($I\bar{4}$) are typical NLO crystals built up with tetrahedral octupolar entities.[8] A class of tetrahedral ions such as tetraphenylphosphonium, -arsonium, and -stibonium has attracted our attention.[9] The octupolar symmetry of these ionic species and their frequent noncentrosymmetric assemblies through the persistence of symmetry operator $\bar{4}$ in numerous crystal structures point out this class of cations as building blocks for an engineering route of octupolar NLO crystals.[10] In addition, the positive charge at P^+ in the phosphonium salts is useful as an electron-withdrawing center for the charge-transfer properties. To our knowledge only one paper has reported the NLO properties of three-dimensional tetraarylphosphonium chromophores, but without studying their arrangement in the solid state.[11] In fact the NLO activity of noncentrosymmetric crystals reported by Lloyd and Brock[9,10] was thought to be feeble due to the lack of donor groups grafted on the tetraphenylphosphonium moiety. Our aim was to check the potential quadratic NLO efficiency of crystals built with tetrahedral tetraarylphosphonium cations having better charge-transfer properties, while remaining transparent in all or nearly all the visible range. We report here after the synthesis, modeling, crystal structure determination, and quadratic nonlinear optical properties of tetra(4-methoxyphenyl)phosphonium iodide or tetraanisylphosphonium iodide, abbreviated as PAn_4I and further called MOPPI, as representative of a new class of octupolar organic nonlinear optical crystals.

Experimental Section

Synthesis. Tris(4-methoxyphenyl)phosphine **1** (1.057 g, 3 mmol), 4-iodoanisole (0.702 g, 3 mmol), and palladium acetate (0.014 g, 0.06 mmol) were stirred in 5 mL of deoxygenated xylene and gradually heated to 140 °C under argon for 20 h. The reagents quickly dissolved, and then a dark oil separated from the solution that solidified on cooling. The brown crude product was recovered by filtration and washed with hot xylene. Purification by column chromatography on silica gel (CH_2Cl_2/AcOEt/MeOH 50:45:5) followed by recrystallization from CH_2Cl_2/AcOEt gave MOPPI as white crystals. The overall yield was 77%. Mp = 213 °C. ^{1}H NMR (200 MHz, $CDCl_3$): δ = 7.50 (dd, J_{HH} = 8.9 Hz, J^3_{HP} = 12.2 Hz), 7.23 (dd, J_{HH} = 8.9 Hz, J^5_{HP} = 2.7 Hz), 3.96 (s, OCH_3). $C_{28}H_{28}IO_4P$ (586.41): Calcd C 57.35, H 4.81; Found C 57.28, H 4.84.

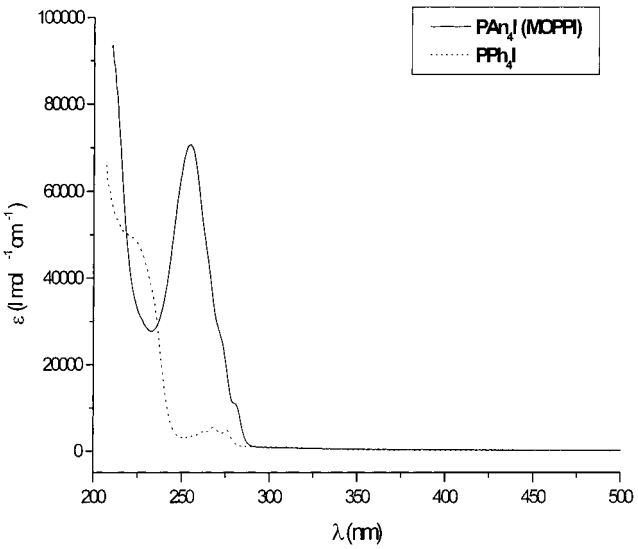

Figure 1. UV−visible spectra of PAn_4I (MOPPI) and PPh_4I in methanol ($c = 2 \times 10^{-5}$ M).

Computational Calculations. All calculations have been performed on a 4 CPU Origin 200 server and an Indigo^2 workstation from Silicon Graphics, using MSI's InsightII software.

SHG Powder Test. The NLO efficiencies of MOPPI and tetraphenylphosphonium iodide were evaluated by the Kurtz and Perry powder test.[12] Noncalibrated freshly crystallized material was used for the second-harmonic generation experiment. The fundamental beam was emitted by a Q-switched, mode-locked Nd^{3+}:YAG laser operating at 1.06 μm, and generating pulse trains at 10 Hz repetition rate. The pulse duration was ~10 ns and fluence of 400mJ/cm^2. The NLO efficiency was evaluated by eye by comparison with the signal of crystalline urea having the same average granulometry.

Spectroscopy. *(a) UV−Visible Spectroscopy.* Solutions of 2×10^{-5} M were prepared by dissolving freshly recrystallized PAn_4I or PPh_4I (Aldrich) in methanol. Samples were contained in quartz cells with 1-cm path lengths. A Hitachi UV2000 spectrophotometer with 0.5-nm resolution was used to collect background spectra of the solvent and spectra of solutions. Spectroscopic curves were plotted by using Origin 5 software (Figure 1).

(b) Nuclear Magnetic Resonance Spectroscopy. ^{1}H nuclear magnetic resonance (NMR) spectral data were obtained on a Bruker AC 200 spectrometer; chemical shifts (δ in ppm) are reported downfield from TMS.

Conditions of Crystal Structure Determination. The crystal used for the diffraction studies was 0.37 × 0.35 × 0.125 mm in size. The positive SHG powder test indicates that MOPPI crystals are noncentrosymmetric. The cell parameters, space group, and crystal structure were determined from single-crystal X-ray diffraction data collected with a Kappa CCD-Nonius diffractometer. Crystal data, experimental conditions, and structural refinement parameters are mentioned in Table 3. No absorption correction was applied; only Lorentz and polarization effects were taken into account. The structure was solved by direct methods using SIR 92 program.[13] Full-matrix least-squares refinements were performed on F using the teXsan software.[14] Scattering factors for neutral atoms and

(6) (a) Ledoux, I.; Zyss, J.; Siegel, J. S.; Brienne, J.; Lehn, J.-M. *Chem. Phys. Lett.* **1990**, *172*, 440. (b) Voigt-Martin, I. G.; Gao, Li; Yakimanski, A.; Schulz, G.; Wolff, J. J. *J. Am. Chem. Soc.* **1996**, *118*, 12830.

(7) (a) Thalladi, V. R.; Brasselet, S.; Bläser, D.; Boese, R.; Zyss, J.; Nangia, A.; Desiraju, G. R. *Chem. Commun.* **1997**, 1841. (b) Thalladi, V. R.; Brasselet, S.; Weiss, H. C.; Bläser, D.; Katz, A. K.; Carrell, H. L.; Boese, R.; Zyss, J.; Nangia, A.; Desiraju, G. R. *J. Am. Chem. Soc.* **1998**, *120*, 2563. (c) Thalladi, V. R.; Boese, R.; Brasselet, S.; Ledoux I.; Zyss, J.; Jetti, R. K. R.; Desiraju, G. R. *Chem. Commun.* **1999**, 1639.

(8) Wells, A. F. *Structural inorganic chemistry*, 5th Ed.; Clarindon Press: Oxford, 1984; pp 835 and 126.

(9) Lloyd, M. A.; Brock, C. P. *Acta Crystallogr.* **1997**, *B53*, 773.

(10) Lloyd, M. A.; Brock, C. P. *Acta Crystallogr.* **1997**, *B53*, 780.

(11) Lambert, C.; Schmälzlin, E.; Meerholz, K.; Bräuchle, C. *Chem. Eur. J.* **1998**, *4*, 512.

(12) Kurtz, S. K.; Perry, T. T. *J. Appl. Phys.* **1968**, *39*, 3798.

(13) Altomare, A.; Cascarano, G.; Giacovazzo, C.; Guagliardi, A. *J. Appl. Crystallogr.* **1993**, *26*, 343.

(14) Molecular Structure Corporation. (1997−1998). teXsan for Windows version 1.03. *Single-Crystal Structure Analysis Software*, Version 1.04; MSC: 3200 Research Forest Drive, The Woodlands, TX 77381.

f′, Δ*f′*, *f″*, and Δ*f″* were taken from *International Tables for X-ray Crystallography*, Vol. C.[15]

Results and Discussion

Synthesis. Tris(4-methoxyphenyl)phosphine **1** is commercially available, or can be obtained following a well-established procedure.[16] The corresponding tetraanisylphosphonium iodide can be conveniently prepared by the palladium-catalyzed reaction of 4-iodoanisole with phosphine **1** in refluxing xylene under argon, according to Migita's procedure.[17]

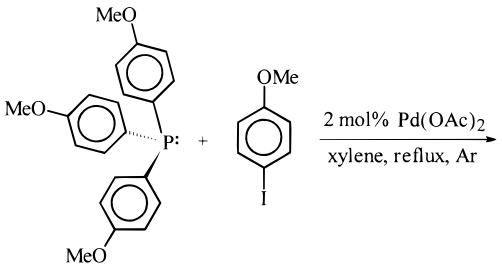

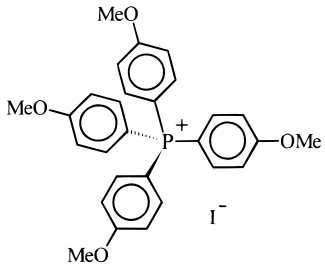

MOPPI

Molecular properties. *Linear Optical Properties.* The absorption spectrum of MOPPI in methanol shows an intense absorption in the UV region ($\lambda_{max} = 255$ nm, $\epsilon = 71\,000$ M^{-1} cm^{-1}) with two small shoulders at the high-energy side of the band (Figure 1). This absorption band corresponds to the donor−acceptor intramolecular charge transfer inside each 4-methoxyphenylphosphonium (PAn_4^+) entity. In comparison the unsubstituted tetraphenylphosphonium cation (PPh_4^+) does not present the same absorption maximum, but only the small peaks corresponding to the shoulders previously reported (Figure 1).

Molecular Modeling. The theoretical structures of PAn_4^+ cation have been computed by the semiempirical AM1 and PM3 Hamiltonians[18] available in MOPAC 6 package and by the ab initio Hartree−Fock based Turbomole software.[19] For the latter, the svp basis[20] has been chosen as a good compromise between accuracy and computational cost. Although it is well-known that many tetraarylphosphonium cations adopt the S_4 conformation in the solid state[10] the isolated PAn_4^+ cation can be optimized either with D_2 or S_4 symmetry (Figure 2). The spatial orientation of the four intramolecular charge-transfer axes remains the same for both symmetries, the main difference coming from the rotation of the benzene rings around these ICT axes. We have defined this rotation by the torsion angle θ, which corresponds to the angle between a benzene ring plane and the P−C bond of a facing ICT axis (Figure 3). Energy comparison between the D_2- and S_4-optimized structures of PAn_4^+ cation evidenced the S_4 conformer as the most stable regardless of the computational methods used. Consequently all the following calculations have been made on the S_4-optimized structures. Selected geometry characteristics are given in Table 1. In the structure optimized by AM1, the P−C bond length is clearly underestimated, at almost 0.20 Å away from the experimental values given here after or from the one in pure S_4 PPh_4^+ cation obtained from the crystal structure of tetraphenylphosphonium iodide.[21] So it appears that the phosphorus parametrization of the AM1 Hamiltonian is not appropriate for phosphonium cations. Better results were obtained with the more recent PM3 Hamiltonian, but the P−C bond length

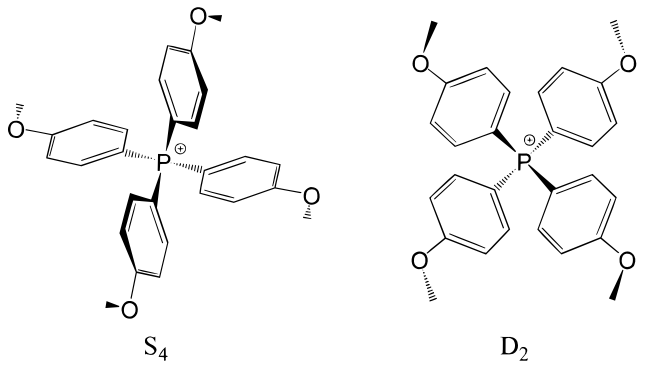

Figure 2. Schematic representation of PAn_4^+ phosphonium cation in S_4 and D_2 symmetry.

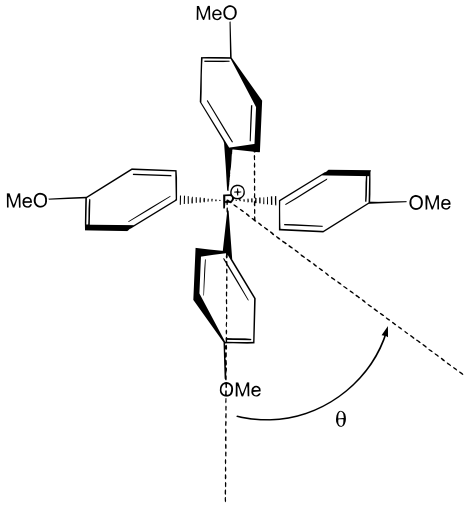

Figure 3. The torsion angle θ drawn in a PAn_4^+ cation in S_4 geometry.

(15) *International Tables for Crystallography*; Wilson, A. J. C., Ed.; Kluwer Academic Publishers: Norwell, MA, 1992; Vol. C, Tables 4268, 6111, 6112.

(16) (a) Friedrischen, B. P.; Powell, D. R.; Whitlock, H. W. *J. Am. Chem. Soc.* **1990**, *112*, 8931. (b) Mann, F. G.; Chaplin, E. J. *J. Chem. Soc.* **1937**, 527.

(17) Migita, T.; Nagai, T.; Kiuchi, K.; Kosugi, M. *Bull. Chem. Soc. Jpn.* **1983**, *56*, 2869.

(18) (a) Dewar, M. J. S.; Zoebisch, E. G.; Healy, E. F.; Stewart, J. J. P. *J. Am. Chem. Soc.* **1985**, *107*, 3902. (b) Stewart, J. J. P. *J. Comput. Chem.* **1989**, *10*, 210.

(19) Ahlrichts, R.; Bär, M.; Häser, M.; Horn, H.; Kölmel C. *Chem. Phys. Lett.* **1989**, *162*, 165.

(20) Schäfer, A.; Horn, H.; Ahlrichts, R. *J. Chem. Phys.* **1992**, *97*, 2571.

(21) Schweizer, E. E.; Baldacchini, C. J.; Rheingold, A. L. *Acta Crystallogr.* **1989**, *C45*, 1236.

Table 1. Comparison between Calculated and Experimental Geometries for PAn_4^+ (Except PPh_4^+ in Last Line)[a]

geometry	P−C bond length	CPC angle	torsion θ	β_{xyz}[b]	β_{xyz}[c]
PAn_4^+ AM1	1.60	109.9−108.7	82.9	8.37	4.23
PAn_4^+ PM3	1.76	109.5−109.3	79.7	8.71	4.54
PAn_4^+ HF/svp	1.81	110.4−107.6	77.6	9.23	4.85
PAn_4^+ crystal	see text	see text	see text	8.10	4.53
PPh_4^+ crystal	1.80	110.4−107.6	63.6	1.81	1.32

[a] All theoretical structures have been optimized in the S_4 symmetry. Bond lengths are given in angstroms, bond angles and torsion θ values in degrees. Second-order hyperpolarizabilities components are static values in 10^{-30} esu. [b] MOPAC-PM3/TDHF values. [c] Turbomole HF/tz2p CPHF values.

remains still 0.04 Å away from its crystallographic value. On the other hand the Turbomole-optimized structure is very close to that observed for PPh_4^+ in the crystal, especially for the P−C bond length and the angles between the ICT axes. As for the torsion angle θ, all the calculated values are all different and quite far from the one observed in the crystal structure of PPh_4I.[21] In fact, this angle appears to be very sensitive to intermolecular interactions since we observe up to 20° of difference between the four θ values (θ = 82.3, 86.8, 66.9, and 68.9° vs 63.6°) inside PAn_4^+ cation in MOPPI crystal. Thus, molecular modeling on an isolated molecule might be not the right way to calculate a correct value of this torsion angle.

Calculations of Nonlinear Optical Properties. Calculations of the hyperpolarizability tensor components of a chromophore necessitate the knowledge of the molecular geometry as accurately as possible. Two ways were investigated: one starting from the previously optimized theoretical structures and the other from the geometry found in the solid state, deduced from X-ray investigations. For the S_4 chromophore, in which the main nonzero component of the second-order hyperpolarizability tensor is β_{xyz}, the classical Finite Field method[22] implemented in MOPAC 6 package cannot be used because this singular component is not calculated. Nevertheless, the static value of β_{xyz} can be obtained with the same AM1 and PM3 Hamiltonians from the time-dependent Hartree−Fock (TDHF) method available in MOPAC 93.[23] The equivalent CPHF (coupled perturbed Hartree−Fock) method has been used for ab initio calculation of β with Turbomole. Kanis et al.[24] have pointed out that the basis size is critical for the accuracy of quantitative second-order hyperpolarizability calculations, and therefore should include diffuse and polarization functions and take electron correlation effects into account. Comparison of the hyperpolarizability values of *p*-nitroaniline (pNA) as a reference molecule, which we have computed with every basis available in Turbomole, led us to choose the tz2p basis instead of svp for properly compute the PAn_4^+ properties. In fact the calculated β_{xxx} value of pNA with tz2p was $\beta_{xxx} = 8.2 \times 10^{-30}$ esu which is close to all those obtained by using larger Turbomole bases, and within the range of accurate Hartree−Fock and second-order Møller−Plesset (MP2) values of the literature.[25] Furthermore, the tz2p basis size was still compatible with acceptable computation times for PAn_4^+ chromophore. The highest tensor components β_{xyz} computed for both calculated and experimental structures are reported in Table 1. First of all we observe that PAn_4^+ hyperpolarizability is greater than that of the unsubstituted PPh_4^+ cation (4.23 to 9.23 × 10^{-30} esu versus 1.32 to 1.81 × 10^{-30} esu). This confirms the reinforced intramolecular charge transfer due to the donor methoxy groups, already evidenced in the UV spectra (Figure 1). For a given geometry of PAn_4^+, the discrepancy between the semiempirical and ab initio calculated β_{xyz} values corresponds to what is usually observed with other chromophores (with a typical ratio of 0.5−0.7). With regard to the theoretical S_4 structures, the PM3/TDHF method appears to be more sensitive to the input geometry than the HF/CPHF does, but both give the highest value on the HF-optimized structure. In addition to the most significant β_{xyz} coefficient, the theoretical S_4-shaped chromophore possesses two other nonzero components β_{xyy} and β_{xzz} related by $\beta_{xyy} = -\beta_{xzz}$ which represent about 1% of β_{xyz}. In the case of the crystalline geometry, the distortion from the pure S_4 symmetry leads to the apparition of many nonvanishing coefficients in the hyperpolarizability β tensor. Nevertheless, this distortion is mainly due to the irregular torsion angle θ induced by the crystal packing, and since the direction of the four intramolecular charge-transfer axes is not

Table 2. Calculated Values of Dipolar and Octupolar Components of β Tensor for PAn_4^+ and PPh_4^+ Cations in Their Solid-State Geometry (in 10^{-30} esu), and the Related Nonlinear Anisotropy ρ

β calculation method	$(\|\|\beta_{J=1}\|\|^2)^{1/2}$	$(\|\|\beta_{J=3}\|\|^2)^{1/2}$	$\rho = \|\|\beta_{J=1}\|\|/\|\|\beta_{J=3}\|\|$
	PPh_4^+		
PM3	0	4.46	∞
HF/tz2p	0	3.25	∞
	PAn_4^+		
PM3	1.13	20.14	17.81
HF/tz2p	0.83	11.18	13.52

Table 3. Crystallographic and Experimental Data

formula	$C_{28}H_{28}O_4PI$
molecular weight	586.41
space group, Z	$P2_12_12_1$, 4
lattice constants (293 K)	a = 10.131(3), b = 10.131(3), c = 25.682(6) Å
V (Å^3), F(000)	2636(1), 1184
μ (mm^{-1})	0.697 (λAg Kα)
D_x (mg m^{-3})	1.478
apparatus	Nonius Kappa CCD, graphite (220) monochromator, 0.5608 Å (Ag Kα)
Bragg angle limit	2° to 20°
	$h = k$ = −11 to 11, l = −30 to 30
scan technique	ϕ scans
scan speed (deg s^{-1})	0.02
scan width (deg)	2
reflections collected	15346
unique data	2550 (Rint = 0.040)
data with $I > 1.2\sigma(I)$	2189
weighting scheme	$w = 1/[\sigma^2(F_o) + 0.00002\ F_o^2]$
no. of parameters	307
R, R_w	0.048, 0.032
largest shift/error	0.001
ρ_{max}, ρ_{min}	0.57, −0.48 e-, Å^3

(22) Kurtz, H. A.; Stewart, J. J. P.; Dieter, K. M. *J. Comput. Chem.* **1990**, *11*, 82.
(23) Karna, S. P.; Dupuis, M. *J. Comput. Chem.* **1991**, *12*, 487.
(24) Kanis, D. R.; Ratner, M. A.; Marks, T. J. *Chem. Rev.* **1994**, *94*, 195.
(25) Sim, F.; Chin, S.; Dupuis, M.; Rice, J. E. *J. Phys. Chem.* **1993**, *97*, 1158.

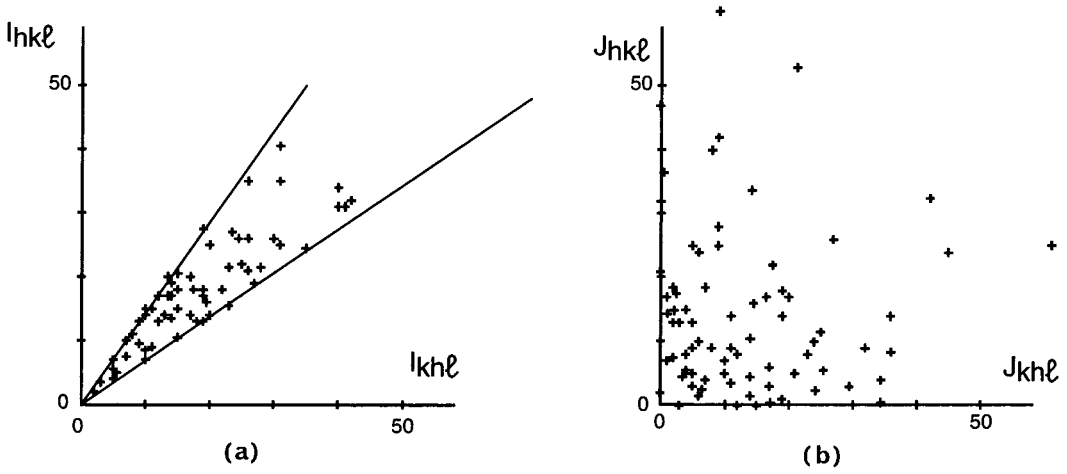

Figure 4. Diagrams of I_{hkl}, J_{hkl} plotted against I_{khl}, J_{khl}: (a) observed intensities for the twinned crystal and (b) observed intensities for the untwinned crystal.

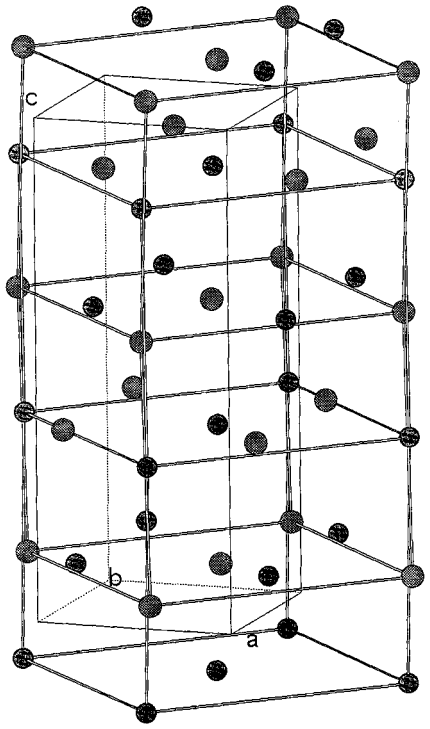

Figure 5. Simplified packing of tetra(4-methoxyphenyl)-phosphonium cations (large spheres) and iodide anions in MOPPI structure evidencing a NaCl-type model.

too far from the pure octupolar S_4 geometry, the β_{xyz} coefficient is still greatly predominant in comparison with all the other ones. Moreover, according to Zyss's definition, the dipolar and octupolar nature of a chromophore is described by the two $\beta_{J=1}$ and $\beta_{J=3}$ spherical components of the β tensor.[3a,b] Calculation of these two components from the computed β_{ijk} Cartesian components clearly shows that $\beta_{J=3} \gg \beta_{J=1}$ (Table 2).[5] Consequently, despite the observed structure distortions (see next section), the PAn_4^+ cation in its crystalline geometry can be considered as a quasi octupolar chromophore in MOPPI crystals.

Crystal structure. *Detection of Twinning and Structure Refinement.* A structural model described with the $P2_12_12_1$ space group established by the diffraction limiting conditions was refined until $R = 0.28$. However

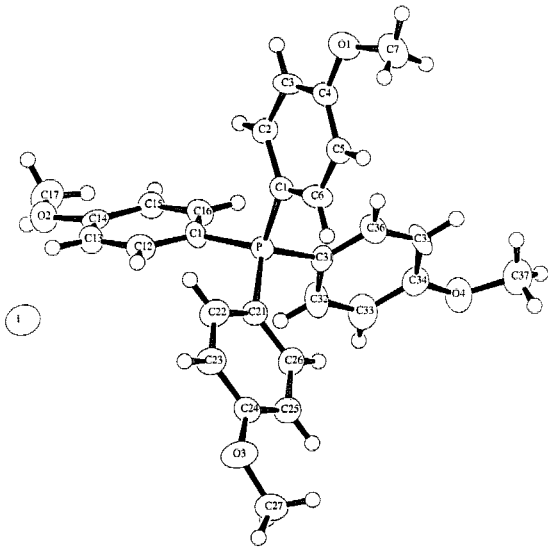

Figure 6. Labeling scheme of the asymmetric unit with displacement ellipsoids at 50% probability level. H atoms are displayed as unlabeled isotropic spheres.

the reliability factor reached the convergence limit and an attempt of refinement of a disordered model did not improve the R value. At this stage, we observed the calculated values I_{hkl} and I_{khl} were very different. The diffracted peaks are not split or diffuse. The observed identity $a = b = 10.131(1)$ Å with acceptable estimated standard deviations indicates that the point symmetry should be $4/m\ 2/m\ 2/m$ (D_{4h}) resulting in following relations for intensity reflections: $I_{hkl} = I_{kh-l} = I_{k-hl} = I_{-khl} = I_{khl} = I_{-hkl} = I_{h-kl} = I_{hk-l}$. The relations and diffraction-limiting conditions observed on all the data show the following:

- The difference between the values of intensities I_{hkl} and I_{khl} is more than the error of measurement (>4%) and then the indice permutation between h and k is not authorized.
- Only the identity $I_{hkl} = I_{-hkl} = I_{h-kl} = I_{hk-l}$ is verified ($R_{\text{int}} = 0.024$).

Consequently these relations are in agreement with the network symmetry mmm. Since the intensities I_{h00}, I_{0k0}, I_{00l} are only observed respectively with $h = 2n$, $k = 2n$, $l = 2n$, the true space group is $P2_12_12_1$.

Table 4. Fractional Atomic Coordinates, Equivalent Displacement Parameters *B*(eq) (Å²) for Non-hydrogen Atoms and Fixed *B*(iso) = 6 Å² for Hydrogen Atoms[a]

atom	*x*	*y*	*z*	*B*(eq)	atom	*x*	*y*	*z*	*B*(eq)	atom	*x*	*y*	*z*	*B*(eq)
I	0.68555(5)	−0.37392(5)	0.60402(2)	4.81(1)	C22	0.3245(7)	−0.1664(6)	0.5664(2)	3.4(1)	H9	0.6749	−0.1324	0.6985	6.000
P	0.2798(1)	0.0582(2)	0.62621(6)	2.51(3)	C23	0.2874(6)	−0.2823(6)	0.5432(3)	3.3(2)	H10	0.5077	0.1575	0.7850	6.000
O1	0.3844(5)	0.4500(4)	0.4607(2)	4.20(12)	C24	0.1611(7)	−0.3331(6)	0.5513(2)	2.9(2)	H11	0.3485	0.1845	0.7213	6.000
O2	0.6981(5)	−0.0229(4)	0.7849(2)	3.82(10)	C25	0.0708(7)	−0.2676(7)	0.5819(3)	3.6(2)	H12	0.7002	−0.0066	0.8604	6.000
O3	0.1360(5)	−0.4490(5)	0.5267(2)	4.65(13)	C26	0.1082(6)	−0.1488(6)	0.6062(3)	3.4(1)	H13	0.7766	0.1055	0.8323	6.000
O4	−0.1952(5)	0.2632(5)	0.7337(2)	4.15(11)	C27	0.0128(8)	−0.5107(7)	0.5372(3)	4.1(2)	H14	0.6234	0.1061	0.8329	6.000
C1	0.3218(6)	0.1655(5)	0.5738(2)	2.43(12)	C31	0.1399(5)	0.1281(7)	0.6590(2)	2.65(12)	H15	0.4113	−0.1316	0.5608	6.000
C2	0.4143(6)	0.2677(6)	0.5814(2)	3.0(1)	C32	0.0923(7)	0.0694(7)	0.7050(3)	4.2(2)	H16	0.3473	−0.3278	0.5214	6.000
C3	0.4317(6)	0.3619(7)	0.5419(3)	3.2(1)	C33	−0.0199(7)	0.1154(9)	0.7287(3)	4.4(2)	H17	−0.0153	−0.3019	0.5871	6.000
C4	0.3597(5)	0.3530(6)	0.4961(2)	2.6(1)	C34	−0.0869(6)	0.2239(7)	0.7081(2)	3.0(2)	H18	0.0475	−0.1030	0.6275	6.000
C5	0.2745(6)	0.2508(7)	0.4881(2)	2.9(1)	C35	−0.0389(7)	0.2825(6)	0.6627(3)	3.7(2)	H19	−0.0017	−0.5144	0.5737	6.000
C6	0.2557(6)	0.1585(6)	0.5271(2)	3.0(2)	C36	0.0744(6)	0.2334(6)	0.6392(3)	3.4(2)	H20	−0.0564	−0.4584	0.5218	6.000
C7	0.2940(8)	0.4696(8)	0.4197(3)	4.7(2)	C37	−0.2844(7)	0.3490(8)	0.7071(3)	4.6(2)	H21	0.0107	−0.5960	0.5228	6.000
C11	0.4121(6)	0.0405(6)	0.6730(2)	2.7(1)	H1	0.4636	0.2740	0.6123	6.000	H22	0.1380	−0.0035	0.7197	6.000
C12	0.5105(6)	−0.0534(6)	0.6666(2)	3.0(1)	H2	0.4936	0.4308	0.5467	6.000	H23	−0.0524	0.0736	0.7591	6.000
C13	0.6060(6)	−0.0690(6)	0.7036(2)	2.9(1)	H3	0.2275	0.2426	0.4562	6.000	H24	−0.0830	0.3564	0.6483	6.000
C14	0.6045(7)	0.0056(7)	0.7489(2)	2.8(1)	H4	0.1966	0.0871	0.5211	6.000	H25	0.1054	0.2736	0.6079	6.000
C15	0.5077(7)	0.1026(7)	0.7550(3)	3.1(2)	H5	0.2095	0.4894	0.4336	6.000	H26	−0.3342	0.3981	0.7313	6.000
C16	0.4141(6)	0.1191(7)	0.7170(2)	3.1(1)	H6	0.3230	0.5409	0.3985	6.000	H27	−0.2360	0.4069	0.6851	6.000
C17	0.6992(8)	0.0531(7)	0.8314(3)	4.5(2)	H7	0.2888	0.3916	0.3992	6.000	H28	−0.3427	0.2972	0.6861	6.000
C21	0.2347(5)	−0.0981(5)	0.5987(2)	2.6(1)	H8	0.5114	−0.1073	0.6361	6.000					

[a] The esd's are in parentheses. $B(\text{eq}) = {}^4/_3 \sum i \sum j \; ai.bj.\beta ij$.

Now if we plot the observed intensities I_{hkl} against I_{khl} (Figure 4a) these are located in a small region of the diagram: a twin of two individuals can explain this nonrandom distribution of intensities. In our case a twin by merohedry is effectively possible or by 90° rotation of the motif around the *c* axis or by effect of a mirror located in the plane (110): since $a = b$, in both cases the intensities of untwinned parts J_{hkl} and J_{khl} are superimposed.[26] To determine the value of the twinning parameter α we have followed the route described by Britton.[27] The two individuals contribute independently to each observed intensity such as

$$I_{hkl} = (1 - \alpha)\, J_{hkl} + \alpha J_{\text{khl}} \text{ and } I_{khl} = (1 - \alpha) J_{khl} + \alpha J_{hkl} \quad (1)$$

J_{hkl} and J_{khl} are the diffracted intensities of an untwinned crystal of same volume as that of the twinned crystal. If α is the fraction of the smaller individual ($\alpha < 0.5$) then the relation $I_{hkl} < I_{khl}$ involves $J_{hkl} < J_{khl}$ and vice versa. From the previous identities the observed intensities of the untwinned crystal can be calculated as

$$J_{hkl} = [(1 - \alpha) I_{hkl} - \alpha I_{khl}]/(1 - 2\alpha) \text{ and } J_{khl} = [(1 - \alpha) I_{khl} - \alpha I_{hkl}]/(1 - 2\alpha) \quad (2)$$

An estimation of α is made from the plot of the Figure 4a.[28] The ratio I_{khl}/I_{hkl} should be situated between $\alpha/1 - \alpha$ and $1 - \alpha/\alpha$. This appears clearly in Figure 4a where all the points are located in a range limited by two lines of respective slopes 0.7 and 1/0.7. The value of α deduced from the slopes is 0.41. J_{hkl} and J_{khl} calculated from observed I_{hkl} and I_{khl} and the value of α were used for crystal structure determination of the untwinned crystal. No correction has been applied to intensities I_{hhl}. A plot of J_{hkl} against J_{khl} shows a random distribution of intensities of the untwinned crystal (Figure 4b).

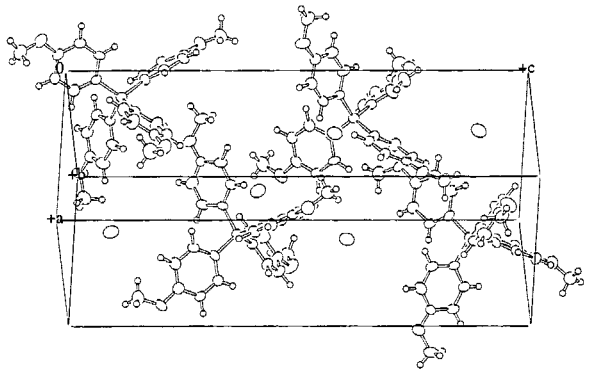

Figure 7. Unit cell of the untwinned MOPPI crystal.

A correction has been also applied to the values $\sigma(I)$. A conventional expression for estimation of error propagation is given by Hamilton[29] for f (x_1, x_2...)

$$\sigma_f^2 = \sum_i (\partial f/\partial x_i)^2 \sigma_{x_i}^2 \quad (3)$$

One can apply relation 3 to obtain $\sigma(J_{hkl})$ (eq 4) and $\sigma(J_{\text{khl}})$ (eq 5):

$$\sigma_{(J_{hkl})}^2 = \left[(1 - \alpha)^2 \sigma_{(I_{hkl})}^2 + \alpha^2 \sigma_{(I_{khl})}^2 + \left(\frac{I_{hkl} - I_{khl}}{1 - 2\alpha}\right)^2 \sigma_\alpha^2\right]/(1 - 2\alpha)^2 \quad (4)$$

$$\sigma_{(J_{khl})}^2 = \left[(1 - \alpha)^2 \sigma_{(I_{khl})}^2 + \alpha^2 \sigma_{(I_{hkl})}^2 + \left(\frac{I_{hkl} - I_{khl}}{1 - 2\alpha}\right)^2 \sigma_\alpha^2\right]/(1 - 2\alpha)^2 \quad (5)$$

In this case $\sigma_\alpha < 0.01$ was neglected.

A program for the calculations of *J* and $\sigma(J)$ from observed intensities, $\sigma(I)$ and α, working with Windows

(26) Friedel, G. *Leçons de Crystallographie*, 2nd ed.; Librairie scientifique Albert Blanchard: Paris, 1964; pp 427−433.
(27) Britton, D. *Acta Crystallogr.* **1972**, *A28*, 296.
(28) Murray-Rust, P. *Acta Crystallogr.* **1973**, *B29*, 2559.
(29) Hamilton, W. C. *Statistics in Physical Sciences*; Ronald Press: New York, 1964.

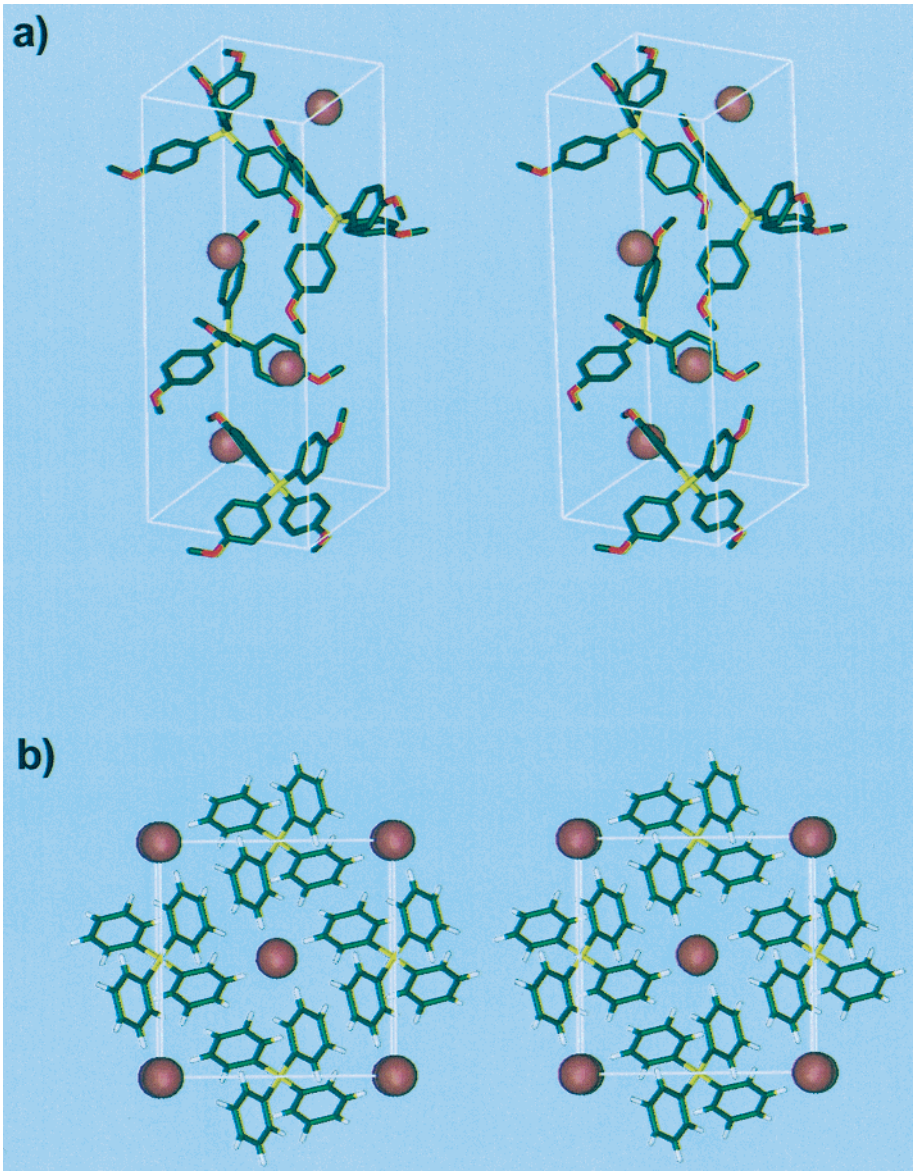

Figure 8. Stereoviews of the unit cells of (a) MOPPI and (b) PPh_4I (atomic coordinates from ref 21).

NT on PC computer, has been written. The refinements were done with successive values of $\alpha = 0.390$, 0.400, 0.402, 0.405, 0.406, 0.408, 0.410, 0.412, and 0.415. The best reliability factors $R = 0.048$, $R_w = 0.032$ were obtained with $\alpha = 0.406$. The crystal structure was drawn using the ORTEP program (Figures 6 and 7) included in teXsan software.[30] Final atomic parameters are listed in Table 4. The main interatomic distances and bond angles are described in Table 5.

Structure Description. If the phosphonium PAn_4^+ cations are represented as large spherical cations the crystal structure of MOPPI can be described as an association of cation and anion fcc subnetworks building a weakly distorted NaCl structure (Figure 5). For the iodide network the cubic cell parameter is precisely the diagonal of the base of the orthorhombic cell. The cation network is however distorted with respect to the anion cubic network. Scrutinizing all the interatomic distances does not evidence any directional interaction between iodide anions and H atoms of the PAn_4^+ cations, showing that MOPPI is actually an ionic compound. On the other hand a network of weak hydrogen bonding between the cations is detected, probably at the origin of the distortion of the cation network. Because of the hydrogen acceptor ability of the oxygen atom belonging to the methoxy group, directional C—H···O bonds between cations are observed (Table 5).[31] Chains of cations are formed through C23—H16···O1 and C7—H5···O3 contacts stretching along the *b* direction. Adjacent chains are linked through C16—H11···O2 and C33—H23···O2 bonds so forming a corrugated layer of cations parallel to the (*a*,*b*) plane. The connection between these layers is completed through C32—H22···O4 and C17—H13···O4 bonds. The geometry of PAn_4^+ cation is tetrahedral (Figure 6). This tetrahedron is not regular (Table 5) and away from $\bar{4}$ symmetry very often observed in many tetraphenylphos-

(30) Johnson, C. K. *ORTEP II*; Report ORNL-5138; Oak Ridge National Laboratory: Oak Ridge, TN, 1976.

(31) (a) Taylor, R.; Kennard, O. *J. Am. Chem. Soc.* **1982**, *104*, 5063. (b) Desiraju, G. R. *Acc. Chem. Res.* **1996**, *29*, 441. (c) Steiner, T. *Acta Crystallogr.* **1995**, *D51*, 93. (d) Steiner, T.; Desiraju, G. R. *Chem. Commun.* **1998**, 891.

Table 5. Selected Interatomic Distances (Å) and Bond Angles (deg) and Their Esd's

Phosphorus Tetrahedral Coordination						
P	C1	1.781(6)	C1	P	C11	112.6(3)
P	C11	1.806(6)	C1	P	C21	107.6(3)
P	C21	1.794(5)	C1	P	C31	107.6(3)
P	C31	1.795(6)	C11	P	C21	111.3(3)
			C11	P	C31	108.2(3)
			C21	P	C31	109.4(3)
Methoxy Groups						
O1	C4	1.362(8)	C4	O1	C7	118.7(5)
O1	C7	1.408(9)	C14	O2	C17	117.6(6)
O2	C14	1.357(8)	C24	O3	C27	117.2(5)
O2	C17	1.421(8)	C34	O4	C37	117.8(5)
O3	C24	1.357(7)				
O3	C27	1.422(9)				
O4	C34	1.339(8)				
O4	C37	1.427(9)				
Phenyl Groups						
C1	C2	1.410(9)	C2	C1	C6	118.8(6)
C1	C6	1.376(9)	C1	C2	C3	118.9(6)
C2	C3	1.404(9)	C2	C3	C4	120.2(6)
C3	C4	1.388(9)	C3	C4	C5	120.2(6)
C4	C5	1.363(9)	C4	C5	C6	119.4(6)
C5	C6	1.383(9)	C1	C6	C5	122.0(6)
			O1	C4	C3	115.1(5)
			O1	C4	C5	124.3(6)
C11	C12	1.388(9)	C12	C11	C16	118.8(6)
C11	C16	1.382(9)	C11	C12	C13	120.3(6)
C12	C13	1.366(9)	C12	C13	C14	120.6(6)
C13	C14	1.386(9)	C13	C14	C15	119.1(6)
C14	C15	1.40(1)	C14	C15	C16	119.4(7)
C15	C16	1.370(9)	C11	C16	C15	121.4(6)
			O2	C14	C13	116.6(6)
			O2	C14	C15	124.3(6)
C21	C22	1.412(9)	C22	C21	C26	119.5(6)
C21	C26	1.394(8)	C21	C22	C23	120.0(6)
C22	C23	1.369(9)	C22	C23	C24	120.2(6)
C23	C24	1.39(1)	C23	C24	C25	121.2(6)
C24	C25	1.37(1)	C24	C25	C26	119.1(6)
C25	C26	1.408(9)	C21	C26	C25	120.0(6)
			O3	C24	C23	114.9(5)
			O3	C24	C25	123.9(6)
C31	C32	1.408(9)	C32	C31	C36	118.6(5)
C31	C36	1.355(9)	C31	C32	C33	120.9(7)
C32	C33	1.37(1)	C32	C33	C34	120.2(7)
C33	C34	1.39(1)	C33	C34	C35	118.8(6)
C34	C35	1.39(1)	C34	C35	C36	119.9(6)
C35	C36	1.389(9)	C31	C36	C35	121.6(6)
			O4	C34	C33	116.6(6)
			O4	C34	C35	124.6(6)

Hydrogen Bonds

D−H···A	D−H	H···A	D···A	angle (deg)
C23−H16···O1	0.95	2.764	3.579(8)	144.8
C33−H23···O2	0.95	2.789	3.495(9)	131.9
C16−H11···O2	0.95	3.005	3.801(8)	142.7
C7−H5···O3	0.95	2.580	3.28(1)	131.3
C32−H22···O4	0.95	2.712	3.632(9)	163.2
C17−H13···O4	0.95	3.009	3.460(9)	110.8

phonium compounds.[10,21,32] The calculated values of angles O1−P−O4 (104.1°), O1−P−O2 (117.2°), O1−P−O3 (108.4°), O3−P−O4 (107.8°), O3−P−O2 (110.7°), O4−P−O2 (108°) compared to corresponding C−P−C bond angles show an imperfect alignment of P, C, and O atoms in each methoxyphenyl group: P, C, and O atoms indicate the direction of charge transfer. The consequence of intercation C−H···O bonds is a weak distortion of the PAn_4^+ cation not compatible with the $\bar{4}$ symmetry or pure octupolar *Td* symmetry, reflected also in the distorted fcc network of cations (Figure 5).

Nonlinear Optical Activity. All relevant evaluation of NLO efficiency of a crystal is depending on the knowledge of $\chi^{(2)}$ tensor coefficients coupled to the phase-matching conditions. Such a study needs a long time and can run only after the crystal growth of high-quality single crystals of large dimensions. For the chemist only a qualitative evaluation of the NLO efficiency is possible based on the Kurtz and Perry powder test.[12] Despite everything this method gives sufficient information to compare the NLO efficiency of a new material with NLO references (∼30% error). In our case we have compared the SHG signals of powder samples of MOPPI with that of urea. The SHG signals of MOPPI crystalline powders are slightly less than 1× urea when they are illuminated by a Nd^{3+}:YAG laser light at 1.064 μm. In comparison, a crystalline powder of tetraphenylphosphonium iodide, which crystallizes in the noncentrosymmetric $I\bar{4}$ space group,[21] shows a significant but more feeble SHG signal (∼ 0.3× urea). Since the hyperpolarizability of PPh_4^+ is much lower than that of PAn_4^+ (Table 1), it could mean that crystal packing in MOPPI is not optimized for an additive contribution of β_{xyz} to $\chi^{(2)}$. This can be seen by comparing both crystal packing as shown in the stereoviews of Figure 8a,b. In Figure 8a we see that the four PAn_4^+ cations are all oriented in different directions, when in Figure 8b we observe that the tetrahedral PPh_4^+ cations are all oriented in the same manner, which is favorable for a better $\chi^{(2)}$ response. The weak SHG signal observed with MOPPI powder samples could be also explained by the fact that the crystals are twinned: this situation alters the coherence length of fundamental and SH waves since the periodic orientation of cation chromophores is continuously modified in the crystal with the twinning fraction α. Most likely powder samples of MOPPI made from untwinned crystals should exhibit a better $\chi^{(2)}$ response in agreement with β_{xyz} calculations.

Conclusion

The studies reported herein illustrate a new approach in the crystal engineering of quadratic NLO materials. MOPPI is a NLO crystal built with quasi octupolar three-dimensional quaternary phosphonium chromophores. The components of the phosphonium second-order hyperpolarizability tensor have been calculated with semiempirical or ab initio methods implemented in commercialy available software. These methods appear now sufficiently powerful to assist efficiently the synthetic chemist in the molecular design of NLO chromophores. However an experimental investigation of the hyperpolarizability of tetraarylphosphonium cations in solution, by the hyper-Rayleigh scattering method (HRS), would be useful for further studies. MOPPI crystallizes in the orthorhombic 222 crystal class (space group $P2_12_12_1$), rather unusual for a quaternary phosphonium salt for which crystals belong most often to the tetragonal $\bar{4}$ class. The structural analysis of the MOPPI compound reveals an ionic structure of NaCl-type weakly distorted. The tetrahedral cation chromophore PAn_4^+ is slightly distorted but

(32) Bogaard, M. P.; Peterson, J.; Rae, A. D. *Acta Crystallogr.* **1981**, *B37*, 1357.

remains not far from pure octupolar symmetry. MOPPI is transparent throughout the visible range, and is moderatly active in second-harmonic generation at 1.064 μm. The improvement of the quadratic NLO efficiency of MOPPI should be obtained with the production of untwinned crystals. New crystals including PAn_4^+ octupolar chromophores taking full profit of the favorable efficiency-transparency tradeoff could be designed with different counteranions.

Acknowledgment. We thank CNRS for financial support.

Supporting Information Available: Table of anisotropic thermal parameters and tables of observed and calculated structure factors for MOPPI (PDF). An X-ray crystallographic file for MOPPI (CIF). This material is available free of charge via the Internet at http://pubs.acs.org.

CM991155C